Microporous Materials

Deutsche Ausgabe: DOI: 10.1002/ange.201600146
Internationale Ausgabe: DOI: 10.1002/anie.201600146

EU-12: A Small-Pore, High-Silica Zeolite Containing Sinusoidal Eight-Ring Channels

*Juna Bae, Jung Cho, Jeong Hwan Lee, Sung Man Seo, and Suk Bong Hong**

Abstract: *Zeolite EU-12, the framework structure of which has remained unsolved during the past 30 years, is synthesized at a specific SiO_2/Al_2O_3 ratio using choline as an organic structure-directing agent, with both Na^+ and Rb^+ ions present. Synchrotron powder X-ray diffraction and Rietveld analyses reveal that the EU-12 structure has a two-dimensional 8-ring channel system. Among the two distinct 8-ring (4.6 × 2.8 and 5.0 × 2.7 Å) channels along c axis, the smaller one interconnects with the sinusoidal 8-ring (4.8 × 3.3 Å) channel along a axis. The other large one is simply linked up with the sinusoidal channel by sharing 8-rings (4.8 × 2.6 Å) in the ac plane. The proton form of EU-12 was found to show a considerably higher ethene selectivity in the low-temperature dehydration of ethanol than H-mordenite, the best catalyst for this reaction.*

While zeolites and related crystalline materials have a wide variety of commercial applications in catalysis, ion exchange, and gas adsorption and separation, their performance is inherently associated with the shape, size, accessibility and/or dimensionality of the crystallographically well-defined cavities and channels. Over the past several decades, therefore, extensive efforts have been devoted to the synthesis of zeolites with novel framework topologies using numerous different organic amines and alkylammonium ions as organic structure-directing agents (SDAs).[1]

Among the organic SDAs studied thus far, the choline (Ch^+, (2-hydroxyethyl)trimethylammonium) ion is interesting because it crystallizes ferrierite (framework type FER) nanoneedles and SSZ-13 (CHA),[2] with Na^+ present, mainly depending on the Na_2O/SiO_2 ratio in the synthesis mixture. Also, zeolite UZM-22 (MEI) containing 3-rings as part of the structure is the phase formed from the strontium aluminosilicate synthesis mixture containing Ch^+.[3] In particular, Ch^+ can direct the synthesis of a new crystalline inorganic-organic material, that is, the framework-bound organic SDA-containing molecular sieve denoted ECR-40C.[4] These results have prompted us to systematically investigate the effects of inorganic gel chemistry on the phase selectivity in this cheap organic SDA-mediated synthesis of zeolites. Here we report the synthesis of zeolite EU-12 in the mixed Ch^+-Na^+-Rb^+ SDA system and its structure determined by synchrotron powder X-ray diffraction (XRD) and Rietveld analyses. EU-12 was first reported by Araya and Lowe in 1986,[5] but its structure has remained unknown until now. We also show that the proton form of this zeolite is quite selective to ethene formation in the low-temperature dehydration of ethanol.

Table 1 lists the representative products obtained using Ch^+ as an organic SDA from aluminosilicate gels with different oxide compositions, which were heated under rotation (60 rpm) at 150 °C for 7 days. These data reveal that the crystallization of EU-12 is very sensitive to both Al and Rb contents in the synthesis mixture. When the $Rb_2O/(Rb_2O + Na_2O)$ ratio in the synthesis mixture was fixed to 0.7, for example, the SiO_2/Al_2O_3 ratio leading to the successful EU-12 formation was found to be 20 only. When using a rubidium aluminosilicate gel with $SiO_2/Al_2O_3 = 10$, however, we always obtained phillipsite (PHI). Also, a further increase of the SiO_2/Al_2O_3 ratio to 40 and ∞ gave PST-9, the structure determination of which is in progress. When keeping the SiO_2/Al_2O_3 ratio in the gel at 20, on the other hand, we were not able to obtain pure EU-12 from synthesis mixtures with $Rb_2O/(Rb_2O + Na_2O) < 0.7$, which is also the case with $Rb_2O/(Rb_2O + Na_2O) > 0.7$. It thus appears that a reasonable amount of lattice negative charges in the gel, together with a certain level of Rb^+ concentration, may exist in the synthesis of EU-12 using Ch^+.

Table 1: Representative synthetic conditions[a] and results.

Run	Gel composition			Product[b]
	SiO_2/Al_2O_3	$M_2O/(M_2O + Na_2O)$	M	
1	6	0.7	Rb	A + edingtonite
2	10	0.7	Rb	phillipsite
3	20	0.7	Rb	EU-12
4	40	0.7	Rb	PST-9
5	∞	0.7	Rb	U
6	20	0.0	Rb	ferrierite + PST-9
7	20	0.3	Rb	EU-12 + U
8	20	0.5	Rb	EU-12 + PST-9
9	20	1.0	Rb	PST-9 + U
10[c]	20	0.7	Rb	sodalite
11	20	0.7	Li	A
12	20	0.7	K	PST-9 + ZSM-34
13	20	0.7	Cs	analcime + U

[a] The oxide composition of the synthesis mixture is $2.0\,ChCl \cdot x\,M_2O \cdot (1-x)\,Na_2O \cdot y\,Al_2O_3 \cdot 5.0\,SiO_2 \cdot 100\,H_2O$, where x and y are varied between $0 \le x \le 1$ and $0 \le y \le 0.83$, respectively, and M is Li, K, Rb, or Cs. All the syntheses were performed under rotation (60 rpm) at 150 °C for 7 days. [b] The product appearing first is the major phase, and A and U indicate amorphous and unknown but dense phases, respectively. [c] Run performed using TMACl instead of ChCl.

[*] J. Bae, J. Cho, J. H. Lee, Dr. S. M. Seo, Prof. S. B. Hong
Center for Ordered Nanoporous Materials Synthesis, School of Environmental Science and Engineering, POSTECH
Pohang 790-784 (Korea)
E-mail: sbhong@postech.ac.kr

Supporting information for this article can be found under: http://dx.doi.org/10.1002/anie.201600146.

According to the original patent of EU-12, this zeolite is reported to crystallize with tetramethylammonium (TMA^+) and Rb^+ ions.[5] As shown in Table 1, however, the replacement of Ch^+ with the equivalent amount of TMA^+ under the conditions where the synthesis of EU-12 proved to be highly reproducible yielded sodalite (SOD). Also, the use of LiOH, KOH, or CsOH instead of RbOH did not give EU-12 at all. Therefore, the structure-directing ability of Ch^+ itself may not be strong enough to dominate the crystallization of this zeolite. EU-12 prepared here typically appears as needles with ca. 1 μm in length and 0.1 μm in diameter and shows an exothermic loss (ca. 6 wt%) around 600°C (see Figure S1 in the Supporting Information). Organic decomposition at such a high temperature suggests that it could contain cavities or channels smaller than 10-rings. The micropore volume of its proton form (H-EU-12) determined by N_2 adsorption is 0.09 $cm^3 g^{-1}$, which, in principle, makes EU-12 fall into the microporosity boundary between channel-based small-pore and medium-pore zeolites.

The synchrotron powder XRD pattern of dehydrated H-EU-12 was successfully indexed as orthorhombic, with $a = 17.89757$ Å, $b = 28.87473$ Å, and $c = 7.46527$ Å. The systematic extinctions were consistent with *Amam* as the best space group. Then, a model for the SiO_2 structure with six symmetry-independent tetrahedral atoms (T-atoms, T = Si or Al) and 14 such O atoms was achieved by direct methods using the program EXPO2014.[6] After being optimized using the program GULP,[7] this model was used as a starting point for the Rietveld refinement of the structure of dehydrated H-EU-12. Final R_{wp} and R_p values of 7.5 and 5.7% were achieved, respectively, and crystallographic data can be found in Table S1. The final atomic positions and selected interatomic distances and angles of dehydrated H-EU-12 are given in Tables S2 and S3, respectively, and the final Rietveld plot is displayed in the Supporting Information in Figure S2. The average T–O bond length (1.596 Å) and average O-T-O and T-O-T angles (109.47 and 156.5°, respectively) were found to be in good agreement with those expected for zeolitic materials.

The framework structure of EU-12 zeolite can be constructed using two composite building units (CBUs), that is, $[5^4]$ (*mor*) and $[4^1 5^2 8^2]$ (*t-kdk*) CBUs, in a manner given in Figure 1. Each *mor* CBU connects to two neighbor *mor* CBUs by sharing 5-ring edges in the opposite direction to form a zigzag chain along the *c* axis. This chain connects to *t-kdk* CBUs by sharing 5-ring edges perpendicular to *c* axis to form the repeating unit of the EU-12 structure. Then, the two repeating units connects to each other via their 8-rings to form

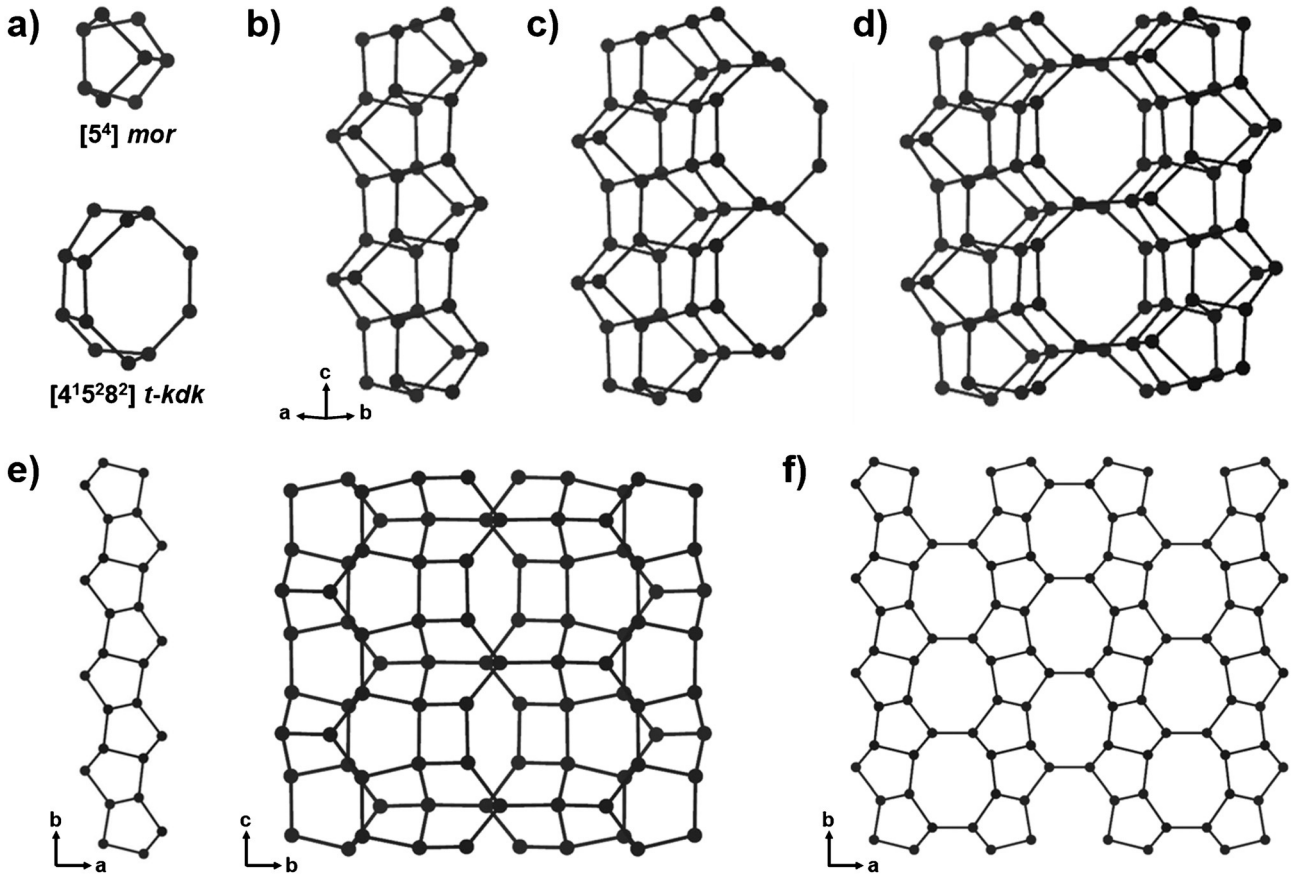

Figure 1. Formation of the EU-12 framework structure. a) $[5^4]$ (*mor*) and $[4^1 5^2 8^2]$ (*t-kdk*) CBUs. b) Connectivity of the *mor* CBU to the other two CBUs by sharing 5-ring edges to form a zigzag chain. c) This chain connects to *t-kdk* CBUs to give the repeating unit of the EU-12 structure. d) The repeating units connect to each other via 8-rings to form e) the EU-12 sheet along the *b* axis. f) Each sheet connects to each other in the *ab* plane via T-O-T linkages to form the EU-12 structure. Bridging O atoms have been omitted for clarity.

a [$4^2 5^4 8^2$-a] (*ygw*) unit,[8] coherently creating the EU-12 sheet. Finally, each sheet extends along the *b* axis and is linked to each other in the *ab* plane via T-O-T linkages across mirror planes that are perpendicular to the *a* axis to complete the framework structure.

As shown in Figure 2, EU-12 has a new unusual framework topology that contains two types of straight 8-ring (4.6 × 2.8 and 5.0 × 2.7 Å) channels along the *c* axis, as well as sinusoidal 8-ring (4.8 × 3.3 Å) channels along the *a* axis. While the smaller 8-ring (Type A) channels intersect with sinusoidal channels, the other larger 8-ring (Type B) channels connect to sinusoidal channels by sharing their 8-rings (4.8 × 2.6 Å) in the *ac* plane. This zeolite is characterized by a framework density (defined as the number of T-atoms per 1000 Å^3) of 18.6, which is relatively high for small-pore materials, mainly due to its channel-based structure. To date, there are only two known small-pore molecular sieves containing sinusoidal channels: thomsonite (THO)[9] and $AlPO_4$-EN3 (AEN).[10] However, thomsonite is not thermally stable when converted into the proton form. This is also the case of $AlPO_4$-EN3 because it transforms into $AlPO_4$-53(C) upon removal of organic SDA molecules by calcination at elevated temperatures.[11]

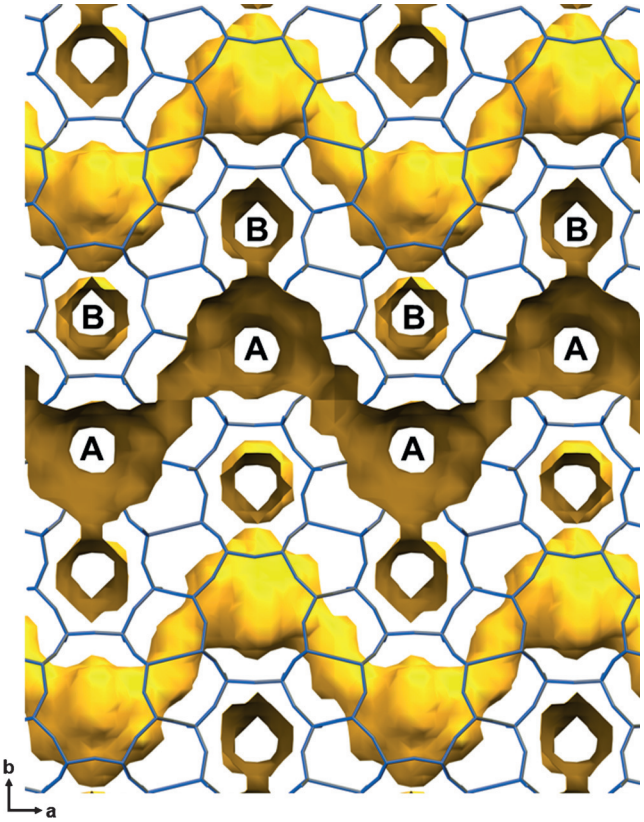

Figure 2. The EU-12 framework structure: the projection down the *c* axis, showing the arrangement of the two types of 8-ring channels, labeled A and B, respectively. Note that while the Type A channels intersect with the sinusoidal channels, the Type B channels link to the sinusoidal ones via their 8-rings.

It is also remarkable that EU-12 is the first zeolite structure with aluminosilicate composition synthesized using Rb^+ ions together with other SDAs.[12] A combination of elemental and thermal analyses reveals that as-made EU-12 has a unit cell composition of $|Rb_{4.7}Na_{0.2}Ch_{3.9}OH_{1.6}(H_2O)_{8.4}|[Al_{7.2}Si_{64.8}O_{144}]$, where OH has been introduced to compensate for the imbalance between the amount of Al and the sum of organic and alkali cations. A negligible amount of Na^+ present suggests that under the synthesis conditions studied here, the presence of Rb^+ itself is the critical factor directing the crystallization of EU-12. Although there is no significant enrichment of Al in the product ($SiO_2/Al_2O_3 = 18$) with respect to the synthesis mixture ($SiO_2/Al_2O_3 = 20$), in addition, the high-silica nature of EU-12 reflects the remarkable stability of its proton form (Figure S3).

The ^{1}H-^{13}C CP MAS NMR spectrum of as-made EU-12 shows only one asymmetrical resonance around 57 ppm, unlike the solution ^{13}C NMR spectrum of Ch^+ in which three resonances are clearly resolved (Figure S4). However, the C/N ratio (4.84) of its organic species determined by CHN analysis is essentially the same as that (5.0) of Ch^+. Moreover, IR spectroscopy manifests the presence of OH groups within organic in as-made EU-12 (Figure S5), showing that Ch^+ remains intact during crystallization of EU-12. Of particular interest is the position (3480 cm^{-1}) of the OH stretching band. This indicates that the occluded Ch^+ ions are involved in intramolecular C-H···O hydrogen bonding,[3b] explaining why the mobility of their CH_2 carbons is considerably lower than that of the CH_3 carbons.

To better understand the intrazeolitic state of Ch^+, we solved the structure of dehydrated as-made EU-12 using powder XRD and Rietveld analyses. As shown in Figure 3, the Ch^+ ion is located in the intersection of the Type A

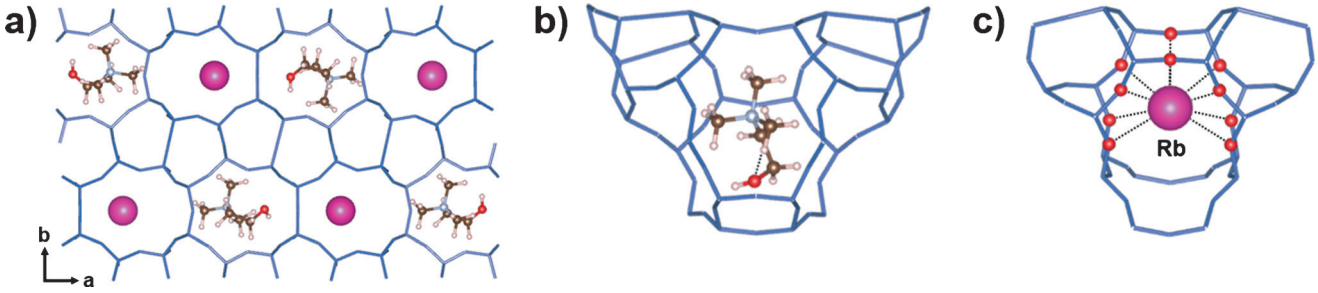

Figure 3. a) Refined structure of dehydrated as-made EU-12 with refined Ch^+ and Rb^+ locations, viewed along the *c* axis. Two possible orientations of the Ch^+ ions are shown. b) [$4^1 5^8 8^5$] and c) [$5^6 6^1 8^3$] cavities containing one Ch^+ site and one Rb^+ position, respectively. Atomic coordinates of hydrogen atoms were electronically optimized at DFT level.

channels and the sinusoidal channels, that is, within the [$4^1 5^8 8^5$] cavities. More interestingly, the O atom of its hydroxyl group is coordinated with the closest C atom of the methyl group at a C···O distance of 2.73 Å (Tables S4 and S5). Consequently, Ch^+ has the gauche conformation stabilized by an intramolecular hydrogen bond. On the other hand, the non-framework Rb^+ ion is located at the off-centered position of [$5^6 6^1 8^3$] cavities that lie in the Type B channels and coordinated with 10 framework O atoms. We note here that among the 14 crystallographically distinct O atoms in the EU-12 framework, only three (i.e., O1, O5, and O12) of them bond with Rb^+ (3.153 ~ 3.392 Å) (Table S5). This is somewhat unexpected because the Rb^+ ion in zeolites is commonly located at the center of the 8-membered ring and prefers to possess coordination numbers of ≤ 8.[13] Since the structure of as-made EU-12 shows an "alternating" arrangement of Rb^+ and Ch^+ locations, therefore, we speculate that EU-12 crystallization may be a result of cooperation between Ch^+ and Rb^+ ions.

Figure 4 compares the catalytic properties of H-EU-12 for ethanol dehydration at 200 °C with those observed for H-ZSM-5 and H-mordenite with similar SiO_2/Al_2O_3 ratios

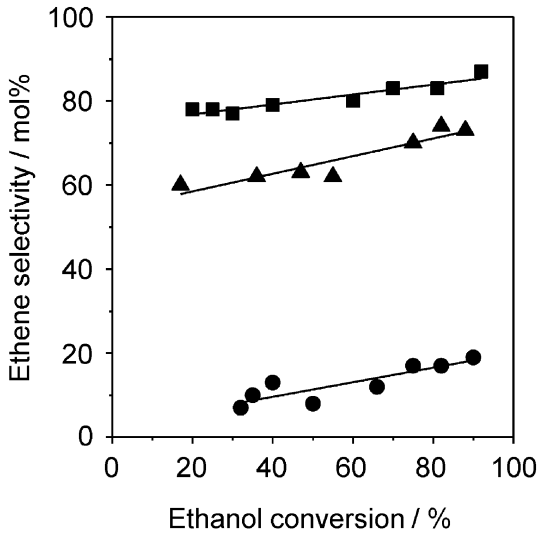

Figure 4. Ethene selectivity as a function of ethanol conversion over H-EU-12 (■), H-ZSM-5 (●), and H-mordenite (▲) at 200 °C with WHSV varied between 0.14 and 21.5 h^{-1}. The only other product observed is diethylether.

(Table S6). We selected this reaction as a probe to characterize the catalytic properties of H-EU-12, because the kinetic diameter (4.5 Å) of ethanol[14] is comparable with the size of EU-12 8-ring pores. Moreover, it is currently of much interest because the dehydration of bioethanol is considered as an alternative route to the production of ethene, the main feedstock in chemical industry.[15] A combination of d_3-acetonitrile IR (Table S6) and NH_3 TPD (Figure S6) measurements reveals that the acid sites in EU-12 have similar density and acid strength to those in the large-pore zeolite H-mordenite, the best catalyst for the low-temperature dehydration of ethanol reported to date.[15a,b] The high ethene selectivity of H-mordenite has been repeatedly shown to originate from the ability of its 8-ring side pockets to effectively isolate the reactant ethanol molecules.

Over the ethanol conversion range (20–90 %) studied, the ethene selectivity of H-EU-12 was found to be always higher by at least 10 % than that of H-mordernite. This strongly suggests that the former zeolite with a multidimensional 8-ring channel system may be more efficient in confining ethanol molecules than the latter one, inhibiting the intermolecular dehydration for diethylether (DEE) formation. The key role of 8-ring channels in the zeolite-catalyzed ethanol dehydration can be further supported by the much lower ethene selectivity of the medium-pore zeolite H-ZSM-5 with two intersecting 10-ring channels (Figure 4). Given that the kinetic diameter (4.2 Å) of ethene is fairly smaller than that (5.4 Å) of DEE,[16] in addition, product shape selectivity seems to govern the reaction over H-EU-12. If such is the case, our work would then be the first example for the shape selective catalysis by channel-based, small-pore zeolites.[17] We also note that for 10 h on stream H-EU-12 is not deactivated at all (Figure S7), revealing the high catalyst stability.

In summary, we have presented the synthesis, structure, and catalytic studies of zeolite EU-12. This material can crystallize only over a particular synthesis mixture composition in the Ch^+-Rb^+-Na^+ mixed-SDA system. EU-12 is a new, small-pore zeolite that contains a 2-dimensional channel system consisting of two types of straight 8-ring (4.6 × 2.8 and 5.0 × 2.7 Å) channels intersected by one type of sinusoidal 8-ring (4.8 × 3.3 Å) ones. Since the Rb^+ ion plays a crucial role in its crystallization, fostering cooperation between this alkali cation and the other type of inorganic and/or organic SDAs in the presence of a certain level of lattice negative charges may be an area of considerable possibility for finding new zeolite structures. H-EU-12 was found to be more selective to ethene in the low-temperature dehydration of ethanol than H-mordenite, the best catalyst for this reaction known thus far.

Acknowledgements

This work was supported by the National Creative Research Initiative Program (2012R1A3A-2048833) through the National Research Foundation of Korea. We thank PAL for synchrotron diffraction beam time. PAL is supported by MSIP and POSTECH.

Keywords: aluminosilicates · ethanol dehydration · microporous materials · structure elucidation · zeolites

How to cite: *Angew. Chem. Int. Ed.* **2016**, *55*, 7369–7373
Angew. Chem. **2016**, *128*, 7495–7499

[1] M. A. Camblor, S. B. Hong in *Porous Materials* (Eds.: D. W. Bruce, D. O'Hare, R. I. Walton), Wiley, Chichester, **2011**, pp. 265–325.

[2] a) Y. Lee, M. B. Park, P. S. Kim, A. Vicente, C. Fernandez, I.-S. Nam, S. B. Hong, *ACS Catal.* **2013**, *3*, 617–621; b) B. Chen, R. Xu, R. Zhang, N. Liu, *Environ. Sci. Technol.* **2014**, *48*, 13909–13916.

[3] a) M. A. Miller, J. G. Moscoso, S. C. Koster, M. G. Gatter, G. J. Lewis, *Stud. Surf. Sci. Catal.* **2007**, *170*, 347 – 354; b) M. B. Park, S. J. Cho, S. B. Hong, *J. Am. Chem. Soc.* **2011**, *133*, 1917 – 1934.
[4] J. K. Lee, J. Shin, N. H. Ahn, A. Turrina, M. B. Park, Y. Byun, S. J. Cho, P. A. Wright, S. B. Hong, *Angew. Chem. Int. Ed.* **2015**, *54*, 11097 – 11101; *Angew. Chem.* **2015**, *127*, 11249 – 11253.
[5] a) A. Araya, B. M. Lowe, US Pat 4581211, **1986**; b) A. Araya, A. J. Blake, I. D. Harrison, H. F. Leach, B. M. Lowe, D. A. Whan, S. P. Collins, *Zeolites* **1992**, *12*, 24 – 31.
[6] A. Altomare, C. Cuocci, C. Giacovazzo, A. Moliterni, R. Rizzi, N. Corriero, A. Falcicchio, *J. Appl. Crystallogr.* **2013**, *46*, 1231 – 1235.
[7] J. D. Gale, A. L. Rohl, *Mol. Simul.* **2003**, *29*, 291 – 341.
[8] S. Han, J. V. Smith, *Acta Crystallogr. Sect. A* **1999**, *55*, 360 – 382.
[9] W. H. Taylor, C. A. Meek, W. W. Jackson, *Z. Kristallogr.* **1993**, *84*, 373 – 398.
[10] J. B. Parise, *Stud. Surf. Sci. Catal.* **1985**, *24*, 271 – 278.
[11] R. M. Kirchner, R. W. Grosse-Kunstleve, J. J. Pluth, S. T. Wilson, R. W. Broach, J. V. Smith, *Microporous Mesoporous Mater.* **2000**, *39*, 319 – 332.
[12] International Zeolite Association, Structure Commission, http://www.iza-structure.org.
[13] a) L. B. McCusker, R. W. Grosse-Kunstleve, C. Baerlocher, M. Yoshikawa, M. E. Davis, *Microporous Mater.* **1996**, *6*, 295 – 309; b) T. Ikeda, K. Itabashi, *Chem. Commun.* **2005**, 2753 – 2755; c) K. Itabashi, A. Matsumoto, T. Ikeda, M. Kato, K. Tsutsumi, *Microporous Mesoporous Mater.* **2007**, *101*, 57 – 65; d) K. Itabashi, T. Ikeda, A. Matsumoto, K. Kamioka, M. Kato, K. Tsutsumi, *Microporous Mesoporous Mater.* **2008**, *114*, 495 – 506.
[14] H. Wu, Q. Gong, D. H. Olson, J. Li, *Chem. Rev.* **2012**, *112*, 836 – 868.
[15] a) H. Chang, A. Bhan, *J. Catal.* **2010**, *271*, 210 – 215; b) T. K. Phung, L. P. Hernández, A. Lagazzo, G. Busca, *Appl. Catal. A* **2015**, *493*, 77 – 89; c) M. E. Potter, M. E. Cholerton, J. Kezina, R. Bounds, M. Carravetta, M. Manzoli, E. Gianotti, M. Lefenfeld, R. Raja, *ACS Catal.* **2014**, *4*, 4161 – 4169.
[16] a) D. Ben-Amotz, K. G. Willis, *J. Phys. Chem.* **1993**, *97*, 7736 – 7742; b) S. Aguado, G. Bergeret, C. Daniel, D. Farrusseng, *J. Am. Chem. Soc.* **2012**, *134*, 14635 – 14637.
[17] a) T. F. Degnan, *J. Catal.* **2003**, *216*, 32 – 46; b) W. Vermeiren, J.-P. Gilson, *Top. Catal.* **2009**, *52*, 1131 – 1161.

Received: January 6, 2016
Revised: March 17, 2016
Published online: May 13, 2016

